

Evaluation of the additional shear demand due to frame-infill interaction: a new capacity model

Original

Evaluation of the additional shear demand due to frame-infill interaction: a new capacity model / Di Trapani, F.; Bogatkina, V.; Petracca, M.; Camata, G.. - In: PROCEDIA STRUCTURAL INTEGRITY. - ISSN 2452-3216. - 44:(2022), pp. 496-503. (Intervento presentato al convegno 19th ANIDIS Conference, Seismic Engineering in Italy tenutosi a ita nel 2022) [10.1016/j.prostr.2023.01.065].

Availability:

This version is available at: 11583/2978851 since: 2023-05-27T07:22:45Z

Publisher:

Elsevier

Published

DOI:10.1016/j.prostr.2023.01.065

Terms of use:

This article is made available under terms and conditions as specified in the corresponding bibliographic description in the repository

Publisher copyright

(Article begins on next page)

XIX ANIDIS Conference, Seismic Engineering in Italy

Evaluation of the additional shear demand due to frame-infill interaction: a new capacity model

Fabio Di Trapani^{a*}, Valentina Bogatkina^b, Massimo Petracca^b, Guido Camata^c

^a*Dipartimento di Ingegneria Strutturale, Edile e Geotecnica, Politecnico di Torino, 10129, Turin, Italy*

^b*ASDEA Software Technology, Via Alide Breviglieri 8, Pescara, Italy*

^c*Department of Engineering and Geology, University of Chieti-Pescara "G. D'Annunzio", Pescara, Italy*

Abstract

During earthquakes, masonry infills exert a significant stiffening and strengthening action which can be favourable or adverse to face the earthquake-induced demand. Infills transfer the force increment to the RC frame members as an additional shear force. Because of this, local shear failures at the end of the columns, or at the end of the beam-column joints can occur. This is particularly true in the case of non-seismically conforming frame structures, as also shown by post-earthquake damage revealed by recent and past earthquakes. Assessment of this additional shear demand is not possible using the common equivalent strut model for the infills. On the other hand, 2D inelastic models are not computationally effective to be used for seismic analysis of large and complex buildings. Because of this, the actual shear demand on columns is underestimated in most cases. In order to maintain the simplicity of the equivalent strut approach without losing the information about the actual shear force on the columns, the current paper provides a detailed study about the infill-frame shear transfer mechanism. Refined 2D inelastic models of real experimental tests on infilled frames have been realized in OpenSees with the aid of the STKO pre and post processor platform. Shear demand on the columns is extracted as an output of the simulations and compared to the axial force resulting from the same simulations made with the equivalent strut models. An analytical relationship allowing estimate the additional shear demand as a function of the current axial force on the equivalent struts and the geometrical and mechanical properties of the infilled frames is finally proposed. The formula can be easily used to perform shear safety checks of columns adjacent to the infills in seismic analyses.

© 2023 The Authors. Published by Elsevier B.V.

This is an open access article under the CC BY-NC-ND license (<https://creativecommons.org/licenses/by-nc-nd/4.0>)

Peer-review under responsibility of the scientific committee of the XIX ANIDIS Conference, Seismic Engineering in Italy.

Keywords: Type your keywords here, separated by semicolons ; infilled frames; shear; reinforced concrete; masonry; OpenSees; STKO.

1. Introduction

Infill-frame interaction has received a special interest by world' researchers since the half of the previous century. Despite the large number of theoretical and experimental studies the interest to this topic is still high. This can be easily recognized, also by an experimental activity, which continued even in last ten years (Da Porto et al. 2013, Cavaleri and Di Trapani 2014, Bergami and Nuti 2015, Verderame et al. 2016, Morandi et al. 2018). Masonry infills

in frame structures influence the response both at the global and the local scale. Global effects include the modification of the overall resistance, stiffness, ductility, and collapse modes (Uva et al. 2012; Fiore et al. 2012; Cavaleri et al. 2017, Di Trapani and Malavisi 2019). On the other hand, local interaction of infills with the frame members also occur. Experimental and numerical studies have in fact shown that infill walls, subject to lateral loads, partially disconnect from the frame, therefore the force transfer is concentrated at the ends of the columns (Fig. 1a), producing a localized increase of shear demand (Koutromanos et al. 2011; Cavaleri and Di Trapani 2015; Caliò and Pantò 2014; Milanesi et al. 2018). The additional shear demand especially affects the column ends and the beam-column joints, jeopardizing the development local brittle failure mechanisms, as many time recognized from post-earthquake damage observation and laboratory tests (Figs. 1b, 1c).

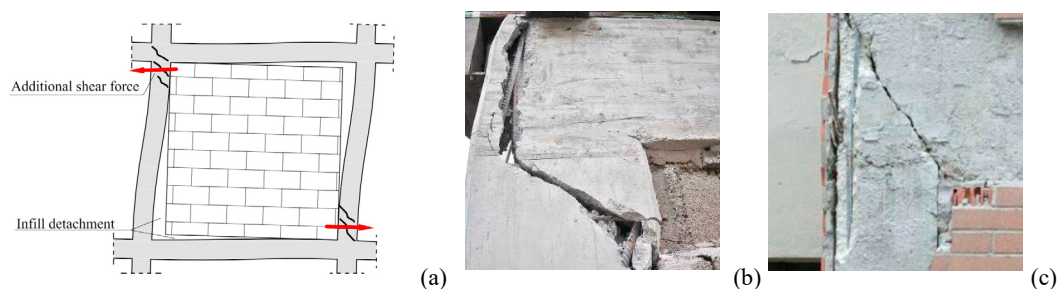


Fig. 1. (a) Local shear interaction of an infilled frame; (b) Shear failure at the end of a column; (c) Shear failure at the end of a column.

Reliable assessment of existing reinforced concrete frame building subject to earthquake loads require the recognition of such kind of potential failure mechanisms. In this framework the evaluation of the additional shear demand due to frame-infill interaction is fundamental to perform timely local safety checks. However, the assessment of the actual shear demand in frame members of infilled frames is not straightforward. On the one hand, finite element micromodels (e.g. Koutromanos et al. 2011, Di Trapani et al. 2018, Di Trapani et al. 2022) are surely the most comprehensive way to simulate frame-infill interaction, although they require a computational effort which is not affordable in practical engineering. On the other hand, the very popular, and computationally effective, equivalent strut approach (e.g. Bertoldi et al. 1993, Panagiotakos and Fardis 1996, Di Trapani et al. 2021) works very well for global analyses, but since equivalent struts have concentric disposition, the additional shear demand is not considered within the internal forces of the frame members. Shear demand is then significantly underestimated when using equivalent struts. Multiple-strut approaches (e.g. Crisafulli et al. 2000, Chrysostomou et al. 2001) have been also proposed from time to time as a potential way to circumvent the problem thanks to the eccentric placement of the struts. The major limitations regard the high sensitivity of the internal forces on the inclination and placement of the struts, besides the calibration of their inelastic response. Based on these premises, this paper proposes a novel methodology to estimate the actual shear demand at the end of the columns adjacent to masonry infills, when using equivalent strut macromodels. In a first step, six real experimental in-plane tests on infilled frames reference have been simulated in with 2D refined FE micromodels using OpenSees (McKenna et al. 2000) with the aid of the STKO platform (Petracca et al. 2021). The FE micromodels were used to numerically extract the shear demand at the ends of the columns. In a second step, the same tests were simulated using the equivalent strut approach. An analytical relationship between the current axial load acting on the equivalent strut and the actual shear demand at the ends of the columns is finally defined. The proposed formula allows performing shear capacity safety checks of columns adjacent to the infills maintaining all the advantages of the simple equivalent strut approach.

2. Refined FE modelling of the infilled frames

2.1. Specimen details

Six in-plane experimental tests on solid masonry infilled frames were selected as reference. Experimental tests were selected from the experimental campaigns by Mehrabi and Shing (1996) and Cavaleri and Di Trapani (2014). The

selection of the specimens was carried with the aim to cover as much as possible the different typologies of masonry within the masonry infills. Specimens 5, 7 and 9 were selected from Mehrabi and Shing (1996). These were made of solid brick masonry (5 and 7) and clay hollow brick masonry (8). Specimens S1A, S1B and S1C by Cavaleri and Di Trapani (2014) were arranged with calcarenite, hollow clay, and light weight concrete masonry units respectively. Moreover, the specimens of two sets had a different aspect ratio (l/h) of the infills. Namely, l/h was 1.43 for Mehrabi and Shing (1996) specimens and 1 for Cavaleri and Di Trapani (2014) specimens. General details about the specimens are provided in Table 1. Mechanical properties of materials are not reported for the sake of space, but they can be easily retrieved from the original papers. Some original pictures of the considered specimens are illustrated in Fig. 2.

Table 1. General detail about the selected specimens.

| Reference | Spec. | Masonry type | Infill length (l) [mm] | Infill height (h) [mm] | l/h [-] | Load on columns [kN on each column] |
|------------------------------|-------|---------------------------|-------------------------------|-------------------------------|--------------|--|
| Mehrabi & Shing (1996) | 5 | Solid clay bricks | 1600 | 1600 | 1.0 | 294 |
| | 8 | Hollow clay bricks | 1600 | 1600 | 1.0 | 294 |
| | 9 | Solid clay bricks | 1600 | 1600 | 1.0 | 294 |
| Cavaleri & Di Trapani (2014) | S1A | Solid calcarenite blocks | 2032 | 1422 | 1.43 | 200 |
| | S1B | Hollow clay blocks | 2032 | 1422 | 1.43 | 200 |
| | S1C | Hollow LW concrete blocks | 2032 | 1422 | 1.43 | 200 |

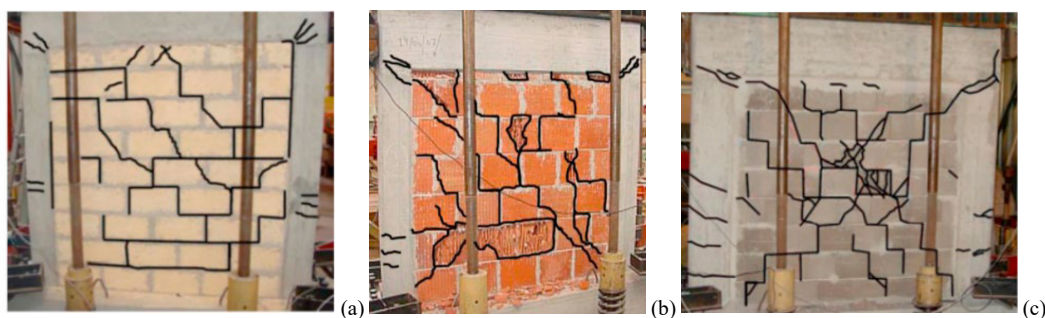


Fig. 2. Some pictures of the specimens and their cracking patterns at the end of the tests: (a) Cavaleri and Di Trapani (2014) Spec. S1A, (b) Cavaleri and Di Trapani (2014) Spec. S1B, (c) Cavaleri and Di Trapani (2014) Spec. S1C.

2.2. Refined FE modelling of the specimens with OpenSees / STKO

Refined micro-modelling of the specimens was carried out using the STKO software platform, which implements OpenSees. Infills and frames were modelled as 2D continuum elements. In detail, both the masonry units and the mortar were modelled as distinct continuum elements (Fig. 3a). For all the 2D elements the *DamageTC3D* constitutive model (Petracca et al. 2011) was used. The latter is based on the continuum damage mechanics, implying the $d+/d-$ tension-compression damage framework. This model introduces two failure criteria for tensile and compressive stress states, as well as two scalar damage indexes, allowing the description of different behaviors under tension and compression. Rebars were modelled as 2D fiber-section elements using the *Steel02* uniaxial material model. Rebars were connected to the 2D concrete frame with an embedded contact element (*ASDEmbeddedNodeElement*) (Fig. 3b). To model this kind of contact, an interaction should be created between concrete and rebars with node-to-element links. In this case the concrete has retained nodes and the reinforcement has constrained nodes. The condition should be assigned to this interaction with a penalty parameter. A penalty stiffness value was used to enforce the constraint of that contact. This value should be high enough to enforce the constraint but not too large otherwise the system may become ill-conditioned. The interface between the RC frame and the infill wall was defined by assigning first a node-to-node interaction (Fig. 3c), then the *ZeroLengthImplexContact* element was used to simulate the contact and frictional response of the interface. Normal and tangential interface stiffness values were calibrated in the analysis starting from reasonable literature values. Friction coefficient was assumed to be 0.7.

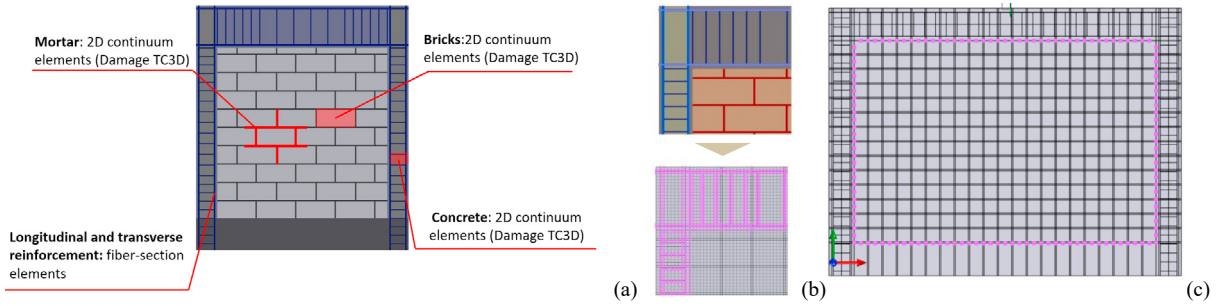


Fig. 3. Refined FE Micro-model of the infilled frame in OpenSees / STKO: (a) Element subdivision; (b) Geometric layout of reinforcement and Node-to-node element links (connection between rebars and frame); (c) Modelling of frame-infill the interface.

2.3. Analysis and model validation

The analysis of the experimental test model was carried out in two steps. First vertical loads were applied at the top of the columns to reproduce the gravity load conditions reported in Table 1. In a second step, a horizontal monotonic increasing displacement is assigned. In Fig. 4, lateral force- lateral displacement curves obtained from the analysis are compared with the positive and negative experimental monotonic envelopes. As it can be observed, numerical responses suitably approximate the average experimental trend in terms of peak resistance, stiffness and post-peak decay. In Fig. 5, experimental and numerical damage patterns are also compared. Also in this case, the numerical model was able to adequately predict the main cracking patterns in the masonry (bricks and mortar joints) as well as in reinforced concrete elements (shear and flexural damage).

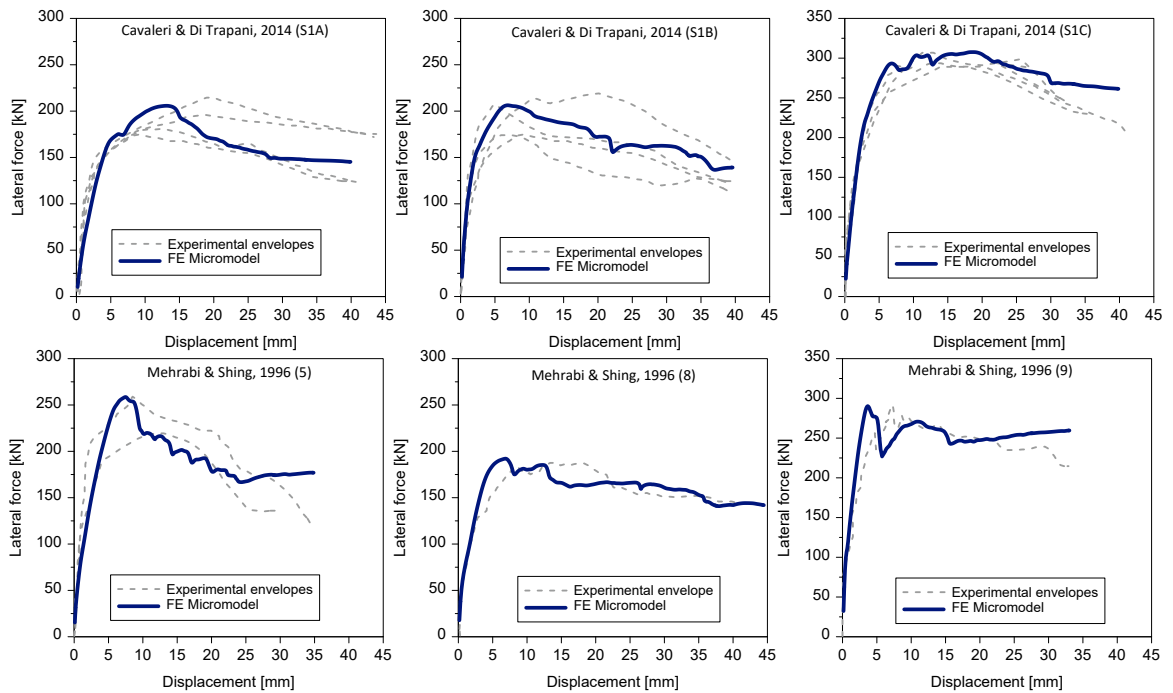


Fig. 4. FE Micromodel experimental / numerical comparisons.

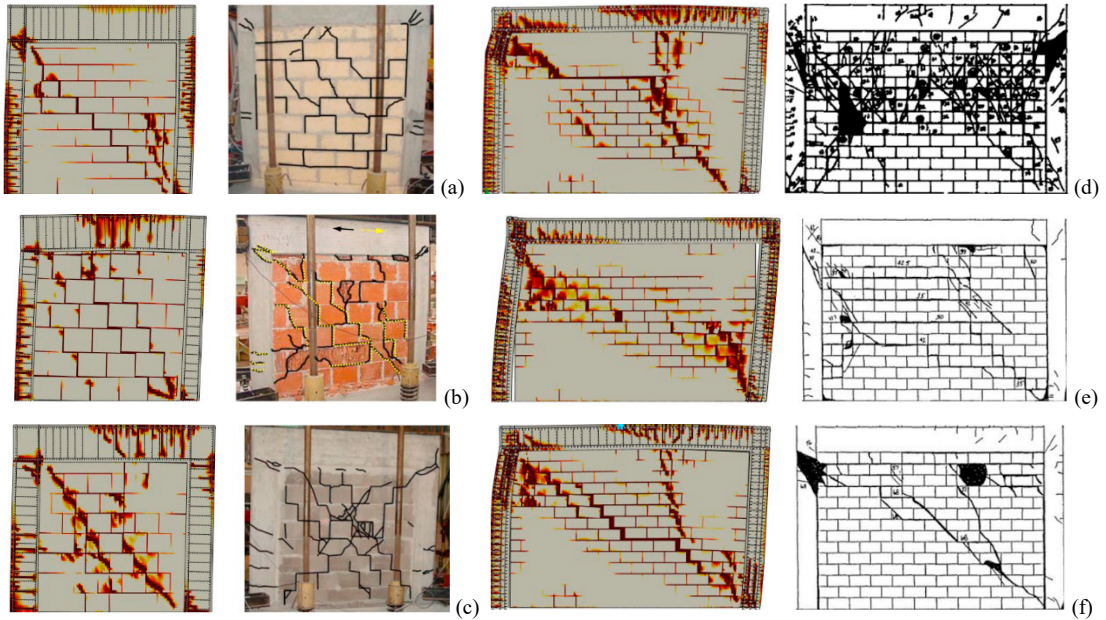


Fig. 5. Comparison between experimental and numerical damage patterns for Cavalieri & Di Trapani (2014) specimens: (a) S1A; (b) S1B; (c) S1C and Mehrabi & Shing (1996) specimens: (d) 5; (e) 8; (f) 9.

3. Numerical assessment of shear demand at the end of the columns due to frame-infill interaction

Shear demand in columns of an infilled frames highly increases at the ends because of the normal stresses transferred by the infill to the column (Fig. 6). In particular, shear diagram assumes a cubic trend in these regions (Cavalieri and Di Trapani 2015), making not univocal the definition of a reference value for shear demand. Because of this, the reference shear demand was conventionally assumed as the average between shear demand values in correspondence of three section cuts made at the extremals and in the middle of the critical region, which supposed to have an extension of $1.5 h_c$, where h_c is the height of the column cross section (Fig. 6). The extraction of the internal forces from the numerical force was carried out by defining a TCL script, that allows specifying the set of nodes where to collect the internal forces and integrating them along the section. Results from this procedure are illustrated in Fig. 7, where the section cut shear demands are plotted for the windward and leeward columns. Average trends are also represented in Fig. 7. It is noteworthy observing that shear demand at the ends of windward and leeward columns is substantially different for the infilled frames having aspect ratio $l/h = 1$, while on the contrary, shear demand is quite similar for the columns in the case of rectangular infilled frames ($l/h = 1.43$). It should be finally observed that the average shear demand approximately coincides with shear demand at the middle cross sections (Cuts 2 and 5).

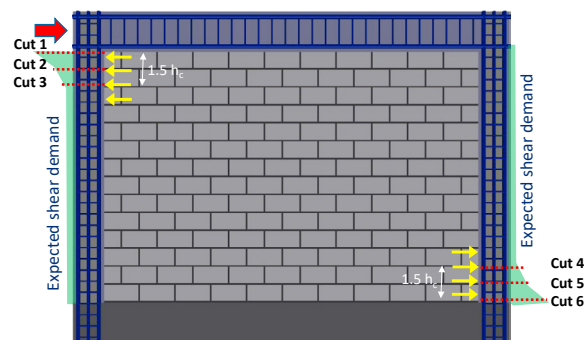


Fig. 6. Decomposition of the total shear demand at the end of the columns of an infilled frame.

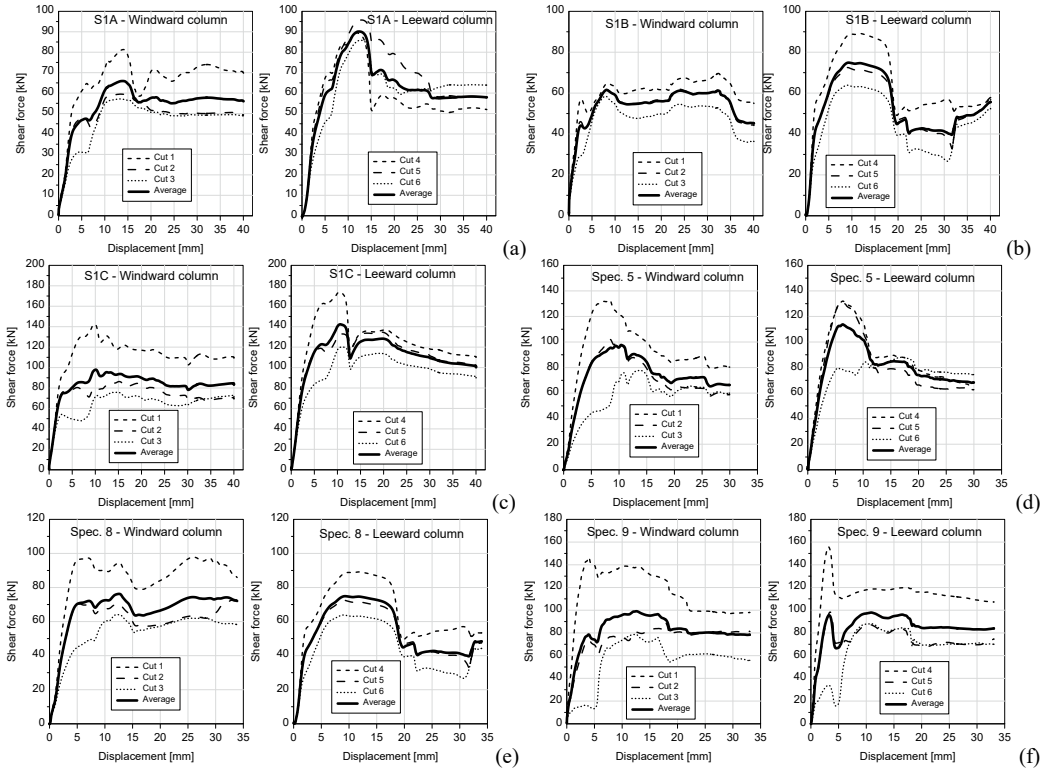


Fig. 7. Total shear demand at the windward and leeward column ends for Cavalieri & Di Trapani (2014) specimens: (a) S1A; (b) S1B; (c) S1C and Mehrabi & Shing (1996) specimens: (d) 5; (e) 8; (f) 9.

4. Prediction of the additional shear demand using macro-modelling approach

Equivalent strut macro-models do not allow assessing local shear demand due to frame-infill interaction. Nevertheless, considering Fig. 8a, it is possible to imagine that the total shear demand at the end of a column adjacent to the infill ($V_{d,tot}$) can be decomposed as the sum of the drift-related shear on the frame ($V_{d,frame}$) and of the additional shear demand due to frame-infill interaction ($V_{d,inf}$), that is:

$$V_{d,tot} = V_{d,frame} + V_{d,inf} \tag{1}$$

While $V_{d,frame}$ is already available as shear internal force from the frame, the term $V_{d,inf}$ is unknown. However it can be reasonably assumed the shear force $V_{d,inf}$ is a rate of the axial force acting on the equivalent strut. In fact, considering the forces acting on a portion of infill at the end of a column, the translational equilibrium equation provides:

$$V_{d,inf} = N \cos \theta - T \tag{2}$$

meaning that the additional shear demand is the difference between the horizontal component of the axial force on the equivalent strut and the tangential friction force at the interface (T). The latter is related to the vertical component (σ_v) of the normal stress acting on the strut (σ_n) through the friction coefficient (μ) and acts on a contact length (al), that is a portion of the total length of the infill (al , with $\alpha \leq l$). The tangential force at the interface is therefore as:

$$T = \mu \sigma_v \cdot t \cdot al \tag{3}$$

where

$$\sigma_v = \sigma_n \sin \theta \quad \text{and} \quad \sigma_n = N / w \cdot t \tag{4}$$

w and t being the width and the thickness of the equivalent strut. Substituting Eq. (4) in Eq. (3) and Eq. 3 in Eq. (2) one obtains:

$$V_{d,inf} = N \cos \theta - \mu \sigma_n \sin \theta \cdot t \cdot \alpha l = N \cos \theta - \frac{\mu \cdot N \sin \theta \cdot t \cdot \alpha l}{w \cdot t} = N \left(\cos \theta - \frac{\mu \cdot \sin \theta \cdot \alpha l}{w} \right) \quad (5)$$

Providing the additional shear demand as a function of the current axial force on the equivalent strut and of the contact length αl . In order to validate the reliability of Eq. (1) combined with Eq. (5), the aforementioned specimens were modelled and analyzed according to the macro-modelling approach proposed by Di Trapani et al. 2018. In Fig. 9, result of the application of the proposed analytical approach are illustrated. In particular, the macro-model predictions of the total shear demand at the ends of the columns are compared with those from the micro-model, showing a noticeable consistency despite the simple approach. As regards the contact length it was assumed $\alpha l=0.30l$ and $0.4l$ for $l/h=1$, and $\alpha l=0.25l$ and $0.3l$ for $l/h=1.5$ for the windward and leeward columns respectively.

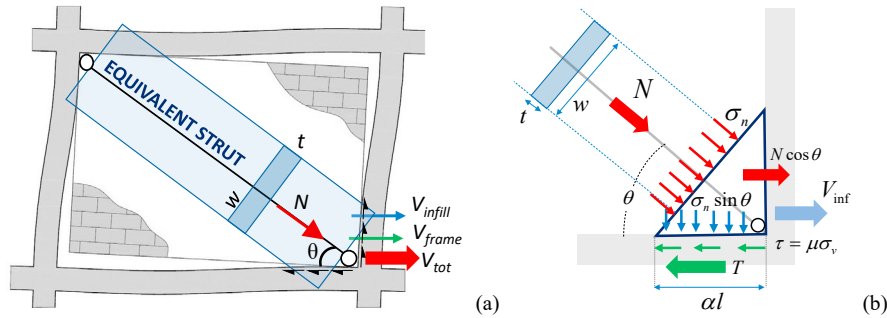


Fig. 8. (a) Decomposition of shear demand at the end of the columns of an infilled frame; (b) Force transfer due to frame-infill interaction.

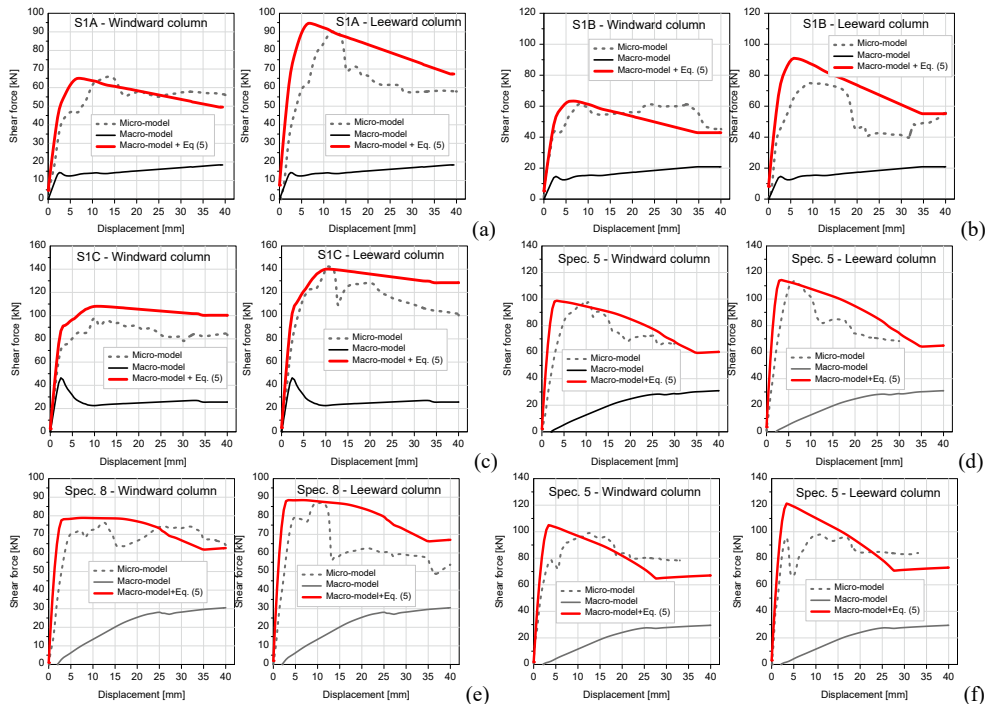


Fig. 9. Comparison between macro-model and micro-model predictions of total shear demand at the windward and leeward column ends for Cavalieri & Di Trapani (2014) specimens: (a) S1A; (b) S1B; (c) S1C and Mehrabi & Shing (1996) specimens: (d) 5; (e) 8; (f) 9.

5. Conclusions

Evaluation of the additional shear demand in RC frame members due to the interaction with the infills is decisive in the assessment of seismic performance of reinforced concrete building subject to earthquake loads. The paper presented a numerical investigation on six infilled frame specimens subject to in plane loads. A refined micromodel realized with OpenSees / STKO, was used to determine the additional shear demand at the end of the columns of these specimens. Subsequently, an analytical formulation was proposed to estimate the additional shear demand using the quite simple and popular equivalent strut approach. Results have shown that the additional shear demand can be related to the current axial force acting on the equivalent strut, and also depend on the effective contact length of the infill with the frame (αl). Preliminary comparisons of the shear demand estimated with the micromodel with that of the micromodel provided quite good results assuming contact length values in the range 0.25l - 0.40l. The proposed model allows performing real time shear safety checks at the end of the columns, maintaining all the advantages of using the equivalent strut approach to analyzed infilled frames. More research is needed to validate the proposed model against a larger dataset of experimental tests and also to provide timely values for the contact lengths having general validity.

Acknowledgements

This paper was supported by DPC-ReLuis 2022–2022, WP10, Subtask 10.1.2 - Non-structural masonry.

References

- Bergami, A.V., Nuti, C., 2015. Experimental tests and global modeling of masonry infilled frames. *Earth Struct* 9(2), 281–303.
- Caliò, I., Pantò, B., 2014. A macro-element modelling approach of Infilled Frame Structures. *Comput Struct* 143, 91–107.
- Cavaleri, L., Di Trapani, F., 2014. Cyclic response of masonry infilled RC frames: experimental results and simplified modeling. *Soil Dyn Earthq Eng* 65, 224–242.
- Cavaleri, L., Di Trapani, F., 2015. Prediction of the additional shear action on frame members due to infills. *Bull Earthq Eng* 13(5), 1425–1454.
- Cavaleri, L., Di Trapani, F., Asteris, P.G., Sarhosis, V., 2017. Influence of column shear failure on pushover-based assessment of masonry infilled reinforced concrete framed structures: A case study. *Soil Dyn Earthq Eng* 100, 98–112.
- Chrysostomou, C.Z., Asteris, P.G., 2012. On the in-plane properties and capacities of infilled frames. *Eng Struct* 41, 385–402.
- Crisafulli, F.J., Carr, A.J., Park, R., 2000. Analytical modelling of infilled frames structures- a general review. *Bull N Z Soc Earthq Eng* 33(1), 30–47.
- da Porto, F., Guidi, M., Dalla Benetta, N., Verlato, F., 2013. Combined in-plane/out-of-plane experimental behaviour of reinforced and strengthened infill masonry walls. 12th Canadian Masonry Symposium, June 2–5, Vancouver, Canada.
- Di Trapani, F., Bertagnoli, G., Gino, D., Ferrotto, M.F., 2018. Empirical equations for the direct definition of stress-strain laws for fiber-section based macro-modeling of infilled frames. *J Eng Mech* 144(11):04018101.
- Di Trapani, F., Malavisi, M., 2019. Seismic fragility assessment of infilled frames subject to mainshock/ aftershock sequences using a double incremental dynamic analysis approach. *Bull Earthq Eng* 17(1), 211–235.
- Di Trapani, F., Vizzino, A., Tomaselli, G., Sberna, A.P., Bertagnoli, G., 2022. A new empirical formulation for the out-of-plane resistance of masonry infills in reinforced concrete frames. *Eng Struct* 266, 114422.
- Fiore, A., Porco, F., Rafaele, D., Uva, G., 2012. About the influence of the infill panels over the collapse mechanisms active under pushover analyses: Two case studies. *Soil Dyn Earthq Eng* 39, 11–22.
- Koutromanos, I., Stavridis, A., Shing, P.B., Willam, K., 2011. Numerical modelling of masonry-infilled RC frames subjected to seismic loads. *Comput Struct* 89, 1026–1037.
- McKenna, F., Fenves, G.L., Scott, M.H., 2000. Open system for earthquake engineering simulation. University of California, Berkeley, CA.
- Mehrabi, A.B., Shing, P.B., Schuller, M.P., Noland, L., 1996. Experimental evaluation of masonry-infilled RC frames. *J Struct Eng (ASCE)* 122(3), 228–237.
- Milanesi, R.R., Morandi, P., Magenes, G., 2018. Local effects on RC frames induced by AAC masonry infills through FEM simulation of in-plane tests. *Bull of Earthq Eng* 16(1), 4053–4080.
- Morandi, P., Hak, S., Magenes, G., 2018. In-plane experimental response of strong masonry infills. *Eng Struct* 156, 503–521.
- Petracca, M., Candeloro, F., Camata, G., 2017. ASDEA Software STKO user manual.
- Petracca, M., Pelà, L., Rossi, R., Zaghi, S., Camata, G., Spacone, E., 2017. Microscale continuous and discrete numerical models for nonlinear analysis of masonry shear walls. *Construction and Building Materials* 149, 296–314.
- Uva, G., Rafaele, D., Porco, F., Fiore, A., 2012. On the role of equivalent strut models in the seismic assessment of infilled RC buildings. *Eng Struct* 42, 83–94.
- Verderame, G.M., Ricci, P., Del Gaudio, C., De Risi, M.T., 2016. Experimental tests on masonry infilled gravity- and seismic-load designed RC frames. In proceedings of 16th international brick and block masonry conference (IBMAC), Padua, Italy.